Int. J. Electrochem. Sci., 7 **(2012)** 8140 - 8150

International Journal of
ELECTROCHEMICAL
SCIENCE
www.electrochemsci.org

Controlled Growth Density and Patterning of Silica Nanorings and Nanowires with Enhanced Ultraviolet Cathodoluminescence Peak

Tung-Hao Chang[1], *Yuan-Chun Lai*[2], *Yu-Cheng Chang*[3,4,*], *Fu-Hsiang Ko*[3], *Fu-Ken Liu*[4,*]

[1] Department of Radiation Oncology, Changhua Christian Hospital, Changhua, 50006, Taiwan
[2] Department of Physics, National Chung Hsing University, Taichung, 40227, Taiwan
[3] Department of Materials Science and Engineering, National Chiao Tung University, Hsinchu, 30010, Taiwan
[4] Department of Applied Chemistry, National University of Kaohsiung, Kaohsiung, 81148, Taiwan
[*]E-mail: ychang0127@gmail.com; fkliu@nuk.edu.tw

Received: 12 June 2012 / *Accepted:* 25 July 2012 / *Published:* 1 September 2012

This study reports the use of monodisperse Au nanoparticles (NPs) as a catalyst for growing silica nanorings (NRs) and nanowires (NWs). Combining spin coating and optical lithography strategies makes it possible to fabricate pattern-monolayer Au NPs that self-assemble on a 3-aminopropyltrimethoxysilane (APTMS)-modified silicon substrate. This can be used as a catalyst for the selective-area growth of silica NRs and NWs. Cathodoluminescence (CL) analysis reveals these NRs and NWs materials exhibit a blue-light emitting phenomenon. The novel optical properties of these materials are advantageous in applications for light-emitting devices with nanoscale dimensions.

Keywords: Nanoparticles; Nanorings; Nanowires; Cathodoluminescence

1. INTRODUCTION

Silica is one of the forms of silicon, which is the second most abundant natural element on earth. Silica generally consists of non-crystallized and disordered atoms [1,2]. Silica material has great technological importance in silicon-based very large scale integrated (VLSI) circuit technology. For example, the application of insulating silica thin films to semiconductor devices has been well-developed for specific tasks, including surface passivation, field effect transistor (FET) gate layer, isolation layers, planarization, and packaging [3]. Silica is also a widely used ceramic material both as a precursor to the fabrication of other ceramic products, and as a material on its own [1].

One-dimensional (1-D) silica nanostructures has received much attention for their applications in nanodevices, including low-dimensional waveguides, scanning near-field optical microscopy, blue light emitters, nanoscale optical devices, and biosensors [3-7]. Silica nanostructures have been fabricated using methods such as thermal evaporation [5], laser ablation [6], sol–gel [8], chemical vapor deposition (CVD) [9], and direct thermal oxidation of Si wafer processes [10-12]. Amount these fabrication strategies, an easy fabrication technique of direct thermal oxidation of Si wafer processes has been demonstrated to grow silica NWs and silica nanocables [11]. Amorphous silica NWs can be grown on a crystalline silicon substrate by first depositing a thin metal film on the substrate surface and then heating it to elevated temperatures in an inert atmosphere containing trace amounts of oxygen [4].

Apart from NWs, researchers have recently shown a great deal of interest in nanometer-sized rings (nanorings, NRs) from theoretical, experimental, and device perspectives [13]. NRs are artificial nanoscale clusters that confine electrons in three dimensions to generate unique physical properties. These properties include persistent currents in metallic [14] or superconducting rings [15], tunable optical resonance in metal rings [16], novel magneto-optical behavior in semiconductor rings [17], magnetic response for applications involving patterned perpendicular recording media [18,19], and novel ring-shaped magneto resistive random access memory (MRAM) [20]. NRs have been fabricated using various methods, including electron beam techniques [2], nanosphere lithography [21], porous alumina template methods [13], DNA template methods [22], particle imprinted template methods [23], and nanomechanical architecture driven by the strain of the Si/Ge layer [24]. However, the ability to develop non-physical deposition techniques, to assemble, and to integrate nanorings into two-dimensional (2D) nanostructure on a substrate remains a challenge.

The self-assembly method, which is an essential part of nanotechnology, is one of the best non-physical deposition techniques for building 2D nanostructures [25]. Previous studies have employed the self-assembly technique utilizing the chemical interaction between NPs and the substrate surface [26]. For example, organic molecules containing thiol (–SH) or amine ($–NH_2$) can be adsorbed on the gold surface to form a well-organized self-assembly monolayer [27]. The self-assembly monolayer process has also been carried out using the immersion method to fabricate a sandwich structure of substrate/organic intermediate/metal NPs [28]. When organizing the sandwich nanostructures, the spin-coating method is far superior to the immersion method for the rapid fabrication of exposed Au NPs attached to APTMS-modified silicon substrate [29,30].

This study reports the successful growth of silica NRs and NWs at specific regions of self-assembled monolayer Au NPs. The spin-coating strategy is a feasible method for controlling the density of self-assembled Au NPs that treated as a catalyst for growing silica NRs on a silicon substrate. Results show that the growth temperature plays an important role in growing silica NRs or NWs. The experiments in this study also employed optical lithography to pattern Au NPs on the substrate and treating them as a catalyst for the selective growth of silica NRs and NWs. Silica NWs exhibit very strong and sharp ultraviolet emission from neutral oxygen vacancies at room temperature. Therefore, the proposed fabrication of large-scale silica NRs or NWs is easy, low cost, and highly efficient, making it conducive to practical light-emitting device applications, and especially in the nanoscale dimension.

2. EXPERIMENT

2.1 Materials and reagents

Sodium citrate, hydrogen tetrachloroaurate($HAuCl_4$), and 3-aminopropyltrimethoxysilane (APTMS) were purchased from Acros (Acros Organics, Geel, Belgium). HPLC grade of ethanol was purchased from J.T. Baker. THMR-ip3650HP resist (TOK, Tokyo, Japan) was employed for I-line exposure. After exposure, the resists could be removed completely after developing with 2.38% tetramethylammonium hydroxide (TMAH, TOK, Tokyo, Japan). De-ionic water (>18 MΩ cm^{-1}) was used throughout the preparation of the Au NPs.

2.2 Growth of silica NRs and NWs

Si (100) wafer were cleaned in a boiling piranha solution (H_2O_2:concentrated H_2SO_4, 3:7, v/v) for 10 min, and then rinsed with de-ionized water and ethanol. The synthesis of Au NPs and their self-assembled on silicon substrate procedures were similar to our previous work [23,24]. Briefly, the Au NPs were self-assembled on 1 cm × 1 cm Si (100) wafer that pre-fabricated with sandwich structure of Si wafer/thin oxide layer/organic amine terminal layer. The silica NRs and NWs were grown by heating of the substrates with self-assembled Au NPs treated as the catalyst at 900 °C or 1050 °C for 1 h in N_2 atmospheric, respectively.

2.3 Apparatus

The morphology of Au NPs and the catalyzed growth of silica NWs on silicon substrate were monitored by a field emission scanning electron microscope (FESEM) using a JEOL JSM-6700F SEM operating at 15 kV accelerating voltage. In addition, a JEOL-2010 transmission electron microscope (TEM) operating at 200 kV was used to monitor the silica nanostructures. The cathodoluminescence (CL) spectra were acquired with an electron probe microanalyzer (Shimadzu EPMA-1500) attached to a SEM. CL spectra were accumulated in a single shot mode with an exposure rate of 1 nm/s. All of the CL spectra were taken at room temperature. An optical lithography (I-line i^{5+} stepper, Canon, Japan) was used for patterning the Au NPs on silicon substrate, which fabrication procedures were the same as described previously [29,30].

3. RESULTS AND DISCUSSION

Figure 1 depicts the method used to fabricate silica NRs. The fabrication processes can be briefly divided into four steps: (1) APTMS-functionalization of the Si substrate, (2) self-assembly of Au NPs on APTMS, (3) catalytic growth of silica NRs on Au, and (4) removal of Au NPs. The first step deposits a large-scale monolayer APTMS on the Si (100) wafer using a thin oxide layer. The second step deposits the Au NPs onto the amino-terminated bonding using a spin-coating method.

After dipping the substrate in a solution of Au NPs, holding for the desired time duration, and spinning out the extra solution using a spin coater at a speed of 1000 rpm, the substrate is immediately rinsed with de-ionized water and dried under a N_2 purge. The third step grows silica NRs by heating the substrates with self-assembled Au NPs at 900 °C for 1 h in a N_2 atmosphere. The fourth step removes the Au NPs by sonicating in de-ionized water for 10 min.

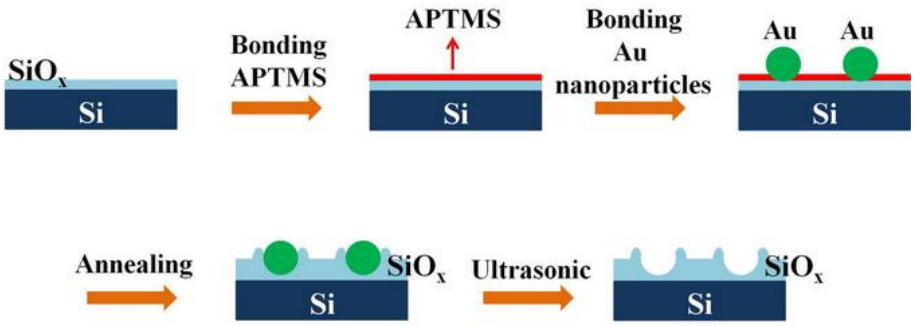

Figure 1. The procedure used to fabricate silica NRs on the silicon substrate.

Figure 2a shows a top-view SEM image of Au NPs self-assembled on the Si substrate. After a deposition period of 10 min, the diameters and density of Au NPs are 10.5 ± 1.9 nm and $1.5x10^2$ per micron^{-2}, respectively. Subsequently, silica NRs were formed at the edge of Au NPs after annealing at 900 °C for 1 h (Fig. 2b). The diameters and density of Au NPs are appreciably changed into 12.7 ± 2.9 nm and $1.4x10^2$ per micron^{-2}, respectively. A comparison of Fig. 2a and b reveals that the Au NPs are significantly different from the original sizes and density. This is probably because neighboring Au NPs start to aggregate, form larger clumps and reducing the density after annealing at 900 °C for 1 h. This can be attributed to the coarsening of the Au structure driven by minimizing the total surface energy [31]. Silica NRs formed well after removing the Au NPs by sonicating in de-ionized water, as shown in the SEM image of Fig. 2c. The high magnification SEM image in the inset image of Fig. 2c shows a concave structure for one of the silica NR. The average outer diameter of a single ring is 16.9 ± 3.8, with an average width of 3-7 nm. The self-assembled bonding between Au NPs and APTMS may fracture under high-temperature annealing, making it easy to remove Au NPs by sonication.

The quantity of Au NPs and silica NRs varies greatly, and increases with increasing holding time of spin coater (Fig. 2d). These results confirm that the holding time of spin coating for Au NPs plays a crucial role in determining the density of Au NPs on the surface of the silicon substrate and the subsequent catalytic growth of silica NRs. In contrast, if there were no Au NPs for catalysis and growth of silica NRs, the futureless structure would appear on the silicon wafer. The results above indicate that spin-coating is an easy method for the density controllable self-assembly of Au NPs and the subsequent catalytic growth of silica NRs on a silicon wafer. Previous NR growth methods cannot change the ring size while effectively controlling the density method [13,21]. The well-defined diameters of Au NPs and spin-coating strategy in this study make it possible to grow different densities of silica NRs with uniform sizes.

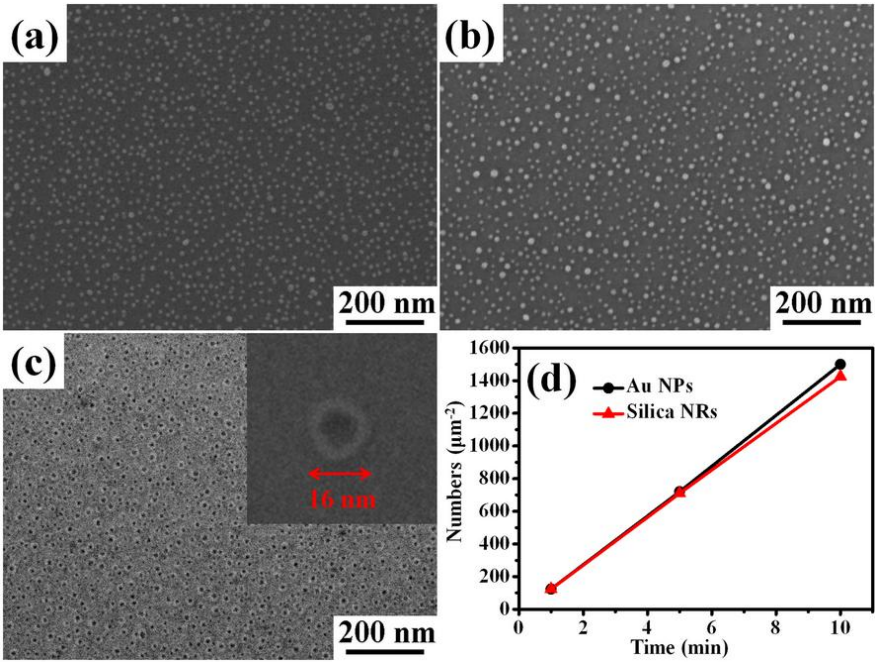

Figure 2. (a) A top-view SEM image of Au NPs were self-assembled on the silicon substrate, (b) annealing at 900 °C for 1 h in a N_2 atmosphere, (c) removing the Au NPs by sonicating in de-ionized water for 10 min. (d) Curve of the deposition time versus the density of the Au NPs and silica NRs.

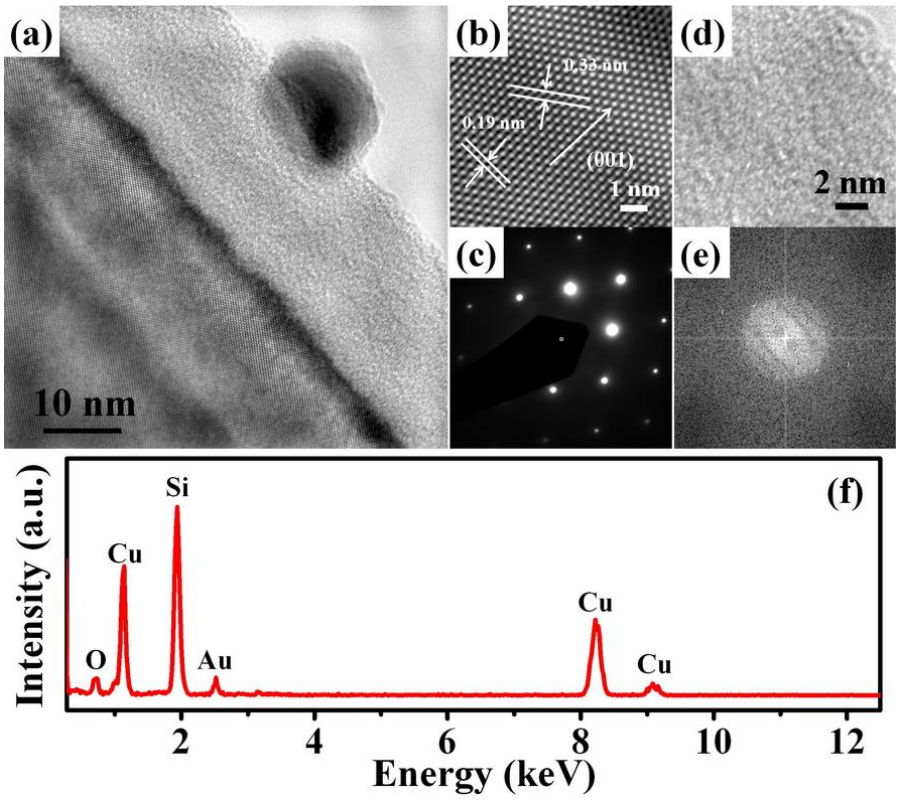

Figure 3. (a) TEM image of an Au NP in Fig. 2b. (b) HRTEM image of the silicon substrate in Fig. 3a. (c) The SAED pattern of the silicon substrate in Fig. 3b. (d) HRTEM image of the silica film in Fig. 3a. (e) The FFT of HRTEM image of the silica film in Fig. 3d. (f) The EDS spectrum of the Au NP in (a).

Figure 3a shows a cross-section TEM image of an Au NP covering silica. The average thickness of silica film is about 20 nm. Figures 3b and c show a high-resolution TEM (HRTEM) image taken from part of the silicon substrate and the corresponding selected-area electron diffraction (SAED) pattern, respectively. The HRTEM image clearly shows single-crystalline lattice fringes along the [010] zone axis. The measured lattice spacings observed in HRTEM are 3.3 and 1.9 Å, which agree with the (101) and (200) lattice spacings of the Si structure, respectively. Both HRTEM image and diffraction pattern reveal that the growth axis of silicon is parallel to the [100] crystallographic direction. Figure 3d shows a HRTEM image of silica film taken from the side section of the silicon substrate. Figure 3e shows a fast Fourier transform (FFT) of the HRTEM image in Fig. 3d. The amorphous phase is further confirmed by FFT (Fig. 3d), which scatters into a halo feature [32]. The EDS spectrum in Fig. 3f reveals the composition of Au NP with a gold component and the compositions of Si and O on the upper layer of the structure. These results confirm that the Au NP is covered with silica.

Figures 4a and b respectively show low and high magnification SEM images of a substrate covered with silica NWs by heating the silicon substrates with self-assembled Au NPs at 1050 °C for 1 h in a N_2 atmosphere. The average diameters and lengths of the silica NWs are approximately 65 ± 4.3 nm and 15.4 ± 1.8 μm, respectively. These results are similar to previous reports. Controlling the size of Au NP catalysts is a remarkable way to control Si NW sizes. Therefore, monodisperse Si NWs were synthesized through the well-defined diameters of Au NPs catalyst using a VLS synthesis strategy [30,33]. The Au NPs in this study also effectively control the growth of silica NWs with uniform sizes. The silica NWs can be directly grown on a silicon substrate, which acts as the silicon source. The growth mechanism is part of a solid-liquid-solid (SLS) method. The SLS growth method is a relatively straightforward way to synthesize silica NWs because it does not require a gas phase precursor.[4] Figure 4c and its inset show TEM image taken from part of an individual silica NW and SAED pattern, respectively. The SAED pattern reveals that the silica NW is of the amorphous phase. The EDS spectrum (Fig. 4d) shows that the elements of Si and O are present in the silica NW. The atomic ratio of Si and O is close to 1:2. Compared with the silica NR in the discussions above, the reaction condition of silica NW differs only in growth temperature. These results confirm that the formation of silica NR or NW is achieved by controlling the adequate reaction temperature.

Researchers have recently spent great efforts on nanopattern assembly and realizing the position-control of Au NPs on solid substrates [34-36]. Some studies have developed rapid and precise selective growth of self-assembled NPs using an electron-beam or optical exposure system with commercial chemically amplified resists [34]. Atomic force microscopy (AFM) was used to locally oxidize the silicon surface and perform the spatially selective deposition of Au NPs via specific chemical interaction [35,36]. In addition, our previous study has reported the fabrication of selectively patterned Au NPs on silicon wafer with the thick silicon oxide film using optical lithography [29]. In the SLS growth method, the thick silicon oxide layer may prevent silicon source evaporation from the silicon wafer. This phenomenon suggests that silica NRs and NWs cannot effectively grow on patterned structures. Therefore, in this present work, the silicon wafer with thin oxide layer was used to grow silica NRs and NWs using an SLS growth mechanism. The patterned structures in this study are

simple to produce, easily controllable, and highly reproducible, making this approach suitable for further studies of nanodevices and their properties.

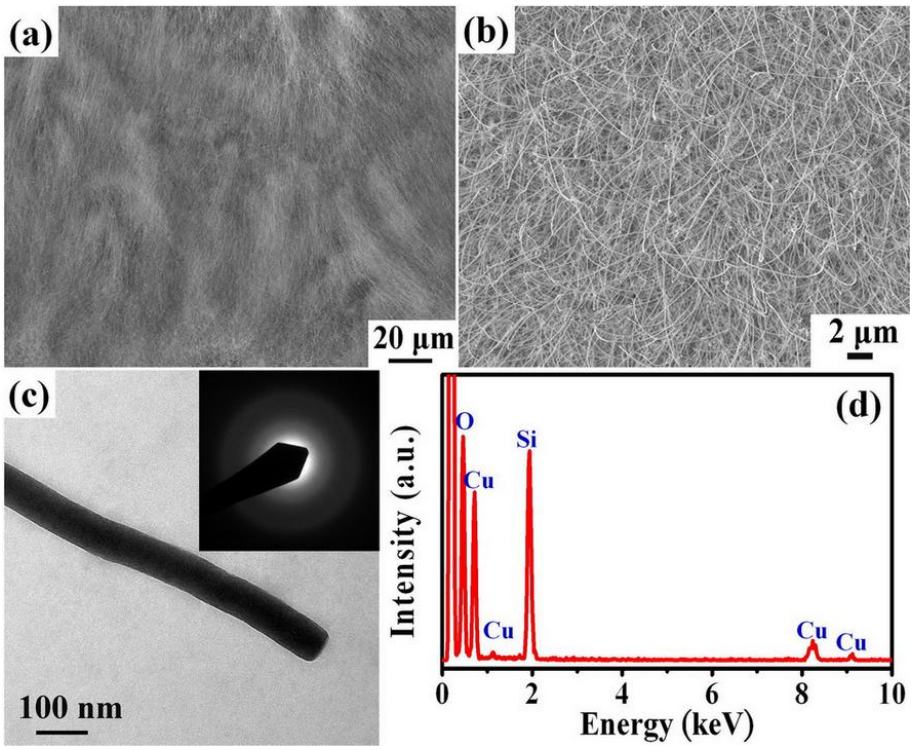

Figure 4. (a) Low and b) high magnification SEM images of the silica NWs grown on the silicon substrate. (c) TEM image and the inert SAED pattern of a silica NW in (a). (d) The EDS spectrum of the NW in (c).

Figures 5a and b respectively show low and high magnification SEM images of a sample with self-assembled Au NPs in an I-line pattern. These figures demonstrate Au NPs grown on selective areas of the silicon substrate, which is ready for the catalytic growth of silica NRs and NWs. Figure 5c shows an SEM image of silica NRs grown on a substrate patterned with the Au NPs shown in Fig. 5a. This pattern can also provide direct evidence to understand the catalytic roles of Au NPs in the silica NRs growth processes. These results further confirm that Au NPs patterns can also control the positions of silica NWs, as shown in Fig. 5d. This study proves that combining optical lithography and spin coating method is a useful approach for fabricating pattern-growth silica NRs or NWs.

Cathodoluminescence is a useful technique for characterizing the optical properties of nanostructures [37]. Since CL uses an electron beam for excitation, it can feasibly to excite only a single or a small group of nanostructures. Thus, this study also employs CL to measure the optical properties of the produced silica NRs and NWs. All of the CL spectra were taken at room temperature. Figure 6a shows a CL spectrum of the silica NRs were grown by heating the silicon substrate with self-assembled Au NPs at 900 °C for 1 h. The weak UV emission appears at approximately 430 nm (2.88 eV). Amorphous silica films are frequently used as passivation or insulation layers in integrated

circuits (IC), and the photoluminescence (PL) properties of various silica glasses have been studied extensively [38]. Nishikawa et al. observed several luminescence bands in various types of high purity silica glasses, with different peak energies ranging from 1.9 to 4.3 eV under 7.9 eV excitation [39]. It was demonstrated that the 2.7 eV (ca. 460 nm) band was ascribed to the neutral oxygen vacancy. The blue light emission from the silica NRs can be attributed to the neutral oxygen vacancies mentioned above.

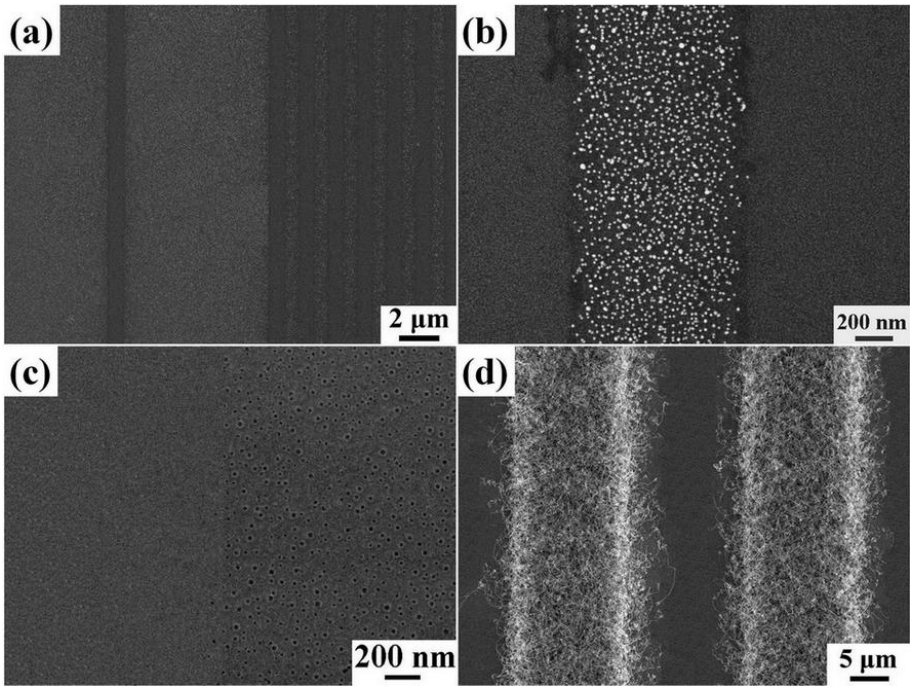

Figure 5. (a) Low and (b) high magnification SEM images of the Au NPs patterned on the silicon substrate. (c) SEM image of silica NRs that were grown on the substrate with patterned Au NPs as shown in (a). (d) SEM image of silica NWs that were grown on the substrate with patterned Au NPs as shown in (a).

Figure 6b shows the CL spectra of silica thin film and silica NWs grown by heating the silicon substrate without and with self-assembled of Au NPs and treated with 1050 °C for 1 h. For silica thin film, a weak UV emission appears at approximately 452 nm (2.74 eV). The thickness of silica thin film is approximately 62 nm (not shown). The CL spectrum from silica NRs with a width of only 3-7 nm and a thin oxide layer produce a 22 nm (0.14 eV) shift in the emission peak. The blue shift is attributed to the quantum confinement effect arising from the reduced size of the widths and thicknesses [37]. For silica NWs, a very sharp and strong peak appears at approximately 454 nm (2.73 eV). Wang et al. reported that the fully oxidized silica NWs have a weak PL peak at approximately 600 nm [40]. Liu et al. showed that two broad PL peaks of SiO_2 were clearly distinguishable at approximately 470 and 420 nm [41]. In addition, Zhu et al. reported two broad PL peaks of SiO_x at approximately 430 and 570 nm [42]. In the current study, the silica NWs emits stable, bright blue light and only one peak at an energy of 2.73 eV. The intensity of the emission is four times higher than that of silica thin film. This extraordinarily intensive blue light emission could be attributed to defect centers of oxygen deficiency

in the wires. The enhancement in only one UV peak optical properties facilitates the application of silica nanowires for nanoscale light-emitting devices.

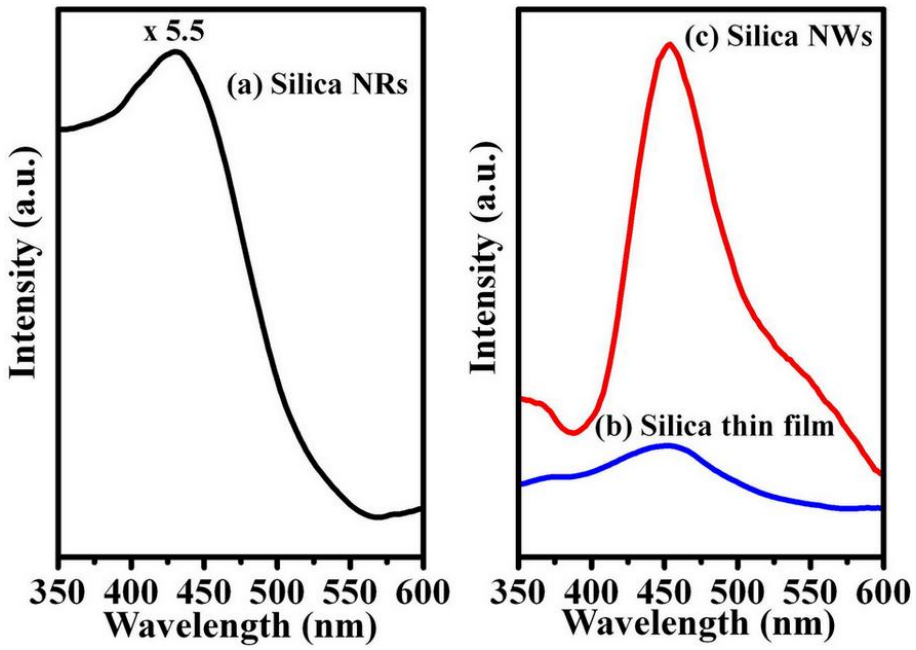

Figure 6. Cathodoluminescence spectra of (a) silica NRs, (b) silica thin film, and (c) silica NWs on the silicon substrate.

4. CONCLUSION

Amorphous silica NRs and NWs were synthesized using direct thermal oxidation of Si wafer processes. The combination of self-assembly monolayer and direct thermal oxidation of Si wafer processes provides a large-scale, easy, and low cost fabrication method that will be of tremendous value in practical applications of growing silica nanodevices. This study combines optical lithography and spin coating method to fabricate Au NPs patterns that can accurately control the positions of silica NRs and NWs. The silica NWs in this study exhibit only one UV emission peak, which is very strong and sharp. The resulting enhancement in UV optical properties is advantageous to applications for nanoscale light-emitting devicesd.

ACKNOWLEDGMENTS
This study was supported financially by the National Science Council, Taiwan (NSC 100-2113-M-390-002-MY3).

References

1. O. G. Palanna, Engineering Chemistry, Tata McGraw-Hill Education Private Limited (2009).
2. A. N. Trukhin, *J. Non-Cryst. Solids* 357 (2011) 1931.

3. Y. Choi, J. L. Johnson, A. Ural, *Nanotechnology* 20 (2009) 135307.
4. C. Y. Wang, L. H. Chan, D. Q. Xiao, T. C. Lin, H. C. Shih, *J. Vac. Sci. Technol*. B 24 (2006) 613.
5. Y. W. Wang, C. H. Liang, G. W. Meng, X. S. Peng, L. D. Zhang, *J. Mater. Chem*. 12 (2002) 651.
6. D. P. Yu, L. Hang, Y. Ding, H. Z. Zhang, Z. G. Bai, J. J. Wang, Y. H. Zou, W. Qian, G. C. Xiong, S. Q. Feng, *Appl. Phys. Lett*. 73 (1998) 3076.
7. D. K. Sood, P. K. Sekhar, S. Bhansali, *Appl. Phys. Lett*. 88 (2006) 143110.
8. W. Bi, R. Song, X. Meng, Z. Jiang, S. Li, T. Tang, *Nanotechnology* 18 (2007) 115620.
9. Z. W. Pan, S. Dai, D. B. Beach, D. H. Lowndes, *Nano Lett*. 3 (2003) 1279.
10. J. Q. Yu, Y. Jiang, X. M. Meng, C. S. Lee, S. T. Lee, *Chem. Phys. Lett*. 367 (2003) 339.
11. B. T. Park, K. Yong, *Nanotechnology* 15 (2004) S365.
12. S. Kar, S. Chaudhuri, *Solid State Commun*. 133 (2005) 151.
13. K. L. Hobbs, P. R. Larson, G. D. Lian, J. C. Keay, M. B. Johnson, *Nano Lett*. 4 (2004) 167.
14. E. M. Q. Jariwala, P. Mohanty, M. B. Ketchen, R. A. Webb, *Phys. Rev. Lett*. 86 (2001) 1594.
15. K. A. Matveev, A. I. Larkin, L. I. Glazman, *Phys. Rev. Lett*. 89 (2002) 096802.
16. J. Aizpurua, P. Hanarp, D. S. Sutherland, M. Ka¨ll, G. W. Bryant, F. J. Garcia de Abajo, *Phys. Rev. Lett.* 90 (2003) 057401.
17. A. Lorke, R. J. Luyken, Jo¨rg P. Kotthaus, A. O. Govorov, J. M. Garcia, P. M. Petroff, *Phys. Rev. Lett.* 84 (2000) 2223.
18. K. Nielsch, R. Hertel, R. B. Wehrspohn, J. Barthel, J. Kirschner, U. Go¨sele, S. F. Fischer, H. Kronmu¨ller, *IEEE Trans. Magnet*. 38 (2002) 2571.
19. S. P. Li, D. Peyrade, M. Natali, A. Lebib, Y. Chen, U. Ebels, L. D. Buda, K. Ounadjela, *Phys. Rev. Lett.* 86 (2001) 1102.
20. J. Zhu, Y. Zheng, G. Prinz, *J. Appl. Phys*. 87 (2000) 6668.
21. A. Kosiorek, W. Kandulski, H. Glaczynska, M. Giersig, *Small* 1 (2005) 439.
22. A. A. Zinchenko, K. Yoshikawa, D. Baig, *Adv. Mater*. 17 (2005) 2820.
23. F. Yan, W. A. Goedel, *Nano Lett*. 4 (2004) 1193.
24. M. Huang, C. Boone, M. Roberts, D. E. Savage, M. G. Lagally, N. Shaji, H. Qin, R. Blick, J. A. Nairn, F. Liu, *Adv. Mater*. 17 (2005) 2860.
25. V. Chechik, R. M. Crooks, C. J. M. Stirling, *Adv. Mater*. 12 (2000) 1161.
26. K. S. Chou, K. C. Huang, H. H. Lee, *Nanotechnology* 16 (2005) 779.
27. F. K. Liu, Y. C. Chang, F. H. Ko, T. C. Chu, B. T. Dai, *Microelectronic Engineering* 67 (2003) 702.
28. W. Li, L. Huo, D. Wang, G. Zeng, S. Xi, B. Zhao, J. Zhu, J. Wang, Y. Shen, Z. Lu, *Colloids Surf*. A 175 (2000) 217.
29. F. K. Liu, P. W. Huang, Y. C. Chang, F. H. Ko, T. C. Chu, *Langmuir* 21 (2005) 2519.
30. T. H. Chang, Y. C. Chang, F. K. Liu, T. C. Chu, *Appl. Surf. Sci*. 256 (2010) 7339.
31. P. Y. Su, J. C. Hu, S. L. Cheng, L. J. Chen, J. M. Liang, *Appl. Phys. Lett*. 84 (2004) 3480.
32. J. H. Kim, Yoon-Uk Heo, A. Matsumoto, H. Kumakura, M. Rindfleisch, M. Tomsic, S. X. Dou, *Supercond. Sci. Technol*. 23 (2010) 075014.
33. A. I. Hochbaum, R. Fan, R. He, P. Yang, *Nano Lett*. 5 (2005) 457.
34. H. L. Chen, Y. H. Chu, C. I. Kuo, F. K. Liu, F. H. Ko, T. C. Chu, *Electrochemical and Solid-State Letters* 8 (2005) G54.
35. J. W. Zheng, Z. H. Zhu, H. F. Chen, Z. F. Liu, *Langmuir* 16 (2000) 4409.
36. S. Hoeppener, R. Maoz, S. R. Cohen, L. Chi, H. Fuchs, J. Sagiv, *Adv. Mater*. 14 (2002) 1036.
37. Y. C. Chang, L. J. Chen, *J. Phys. Chem*. C 111 (2007) 1268.
38. B. B. Li, D. P. Yu, S. L. Zhang, *Phys. Rev*. B 59 (1999) 1645.
39. H. Nishikawa, T. Shiryawa, R. Nakamura, Y. Ohki, K. Nagaswa, Y. Hama, *Phys. Rev.* B 45 (1992) 586.
40. N. Wang, Y. H. Tang, Y. F. Zhang, C. S. Lee, I. Bello, S. T. Lee, *Chem. Phys. Lett*. 299 (1999) 237.

41. D. P. Yu, Q. L. Hang, Y. Ding, H. Z. Zhang, Z. G. Bai, J. J. Wang, Y. H. Zou, W. Qian, G. C. Xiong, S. Q. Feng, *Appl. Phys. Lett*. 73 (1998) 3076.
42. Y. Q. Zhu, W. B. Hu, W. K. Hsu, M. Terrones, N. Grobert, T. Karali, H. Terrones, J. P. Hare, P. D. Townsend, H. W. Kroto, D. R. M. Walton, *Adv. Mater*. 11 (1999) 844.